PT-Symmetric Quaternionic Spacetime: Phenomenological Insights from a String-Inspired Geometric Model

Chien Chih Chen *

Posted Date: 28 May 2025

doi: 10.20944/preprints202503.2052.v2

Keywords: PT symmetry; quaternionic spacetime; dark energy; galactic rotation curves; string theory; non-Hermitian geometry; DBI action; SPARC data

 doi:10.20944/preprints202503.2052.v2

Article

PT-Symmetric Quaternionic Spacetime: Phenomenological Insights from a String-Inspired Geometric Model

Chien-Chih Chen

Chunghwa Telecom Laboratories, Information & Communications Security Laboratory; rocky@cht.com.tw

Abstract: We present a PT-symmetric quaternionic extension of four-dimensional spacetime, in which the metric takes the form $G_{\mu\nu} = g^{(R)}_{\mu\nu} + (\mathbf{i}+\mathbf{j}+\mathbf{k})\, g^{(I)}_{\mu\nu}$. The imaginary component $g^{(I)}_{\mu\nu}$ originates from a coordinate-dependent NS–NS B-field profile $B_{ij} \propto x^k(\mathbf{i}+\mathbf{j}+\mathbf{k})$, motivated by type-IIB flux compactifications with SU(2) gauge symmetry. A concise toy model on flat T^2 demonstrates how a quantized internal flux is mapped, via T-duality and dimensional reduction, into this rotational B-field configuration. A quantitative hierarchy estimate shows that standard string-theoretic ingredients—large-volume suppression, warping, and IR/UV damping— naturally reduce the string-scale value $b_{\text{string}} \sim 10^{70}\,\text{m}^{-2}$ to an effective suppression scale $b_{\text{eff}} \sim 6\times10^{-16}\,\text{m}^{-1}$ consistent with galactic observations. Promoting the quadratic imprint from the DBI determinant to a linear metric correction yields a single dimensionless coupling $\varepsilon \simeq 2.2$ that *simultaneously* (i) reproduces the Planck-2018 dark-energy density $\rho_{\text{imag}} \approx 2.8\times10^{-47}\,\text{GeV}^4$, and (ii) flattens 175 SPARC rotation curves with a reduced $\tilde{\chi}^2_{\text{tot}} \approx 446$, outperforming a three-parameter ΛCDM halo in ∼40% of the sample. The model is linearly stable (ghost- and gradient-free), preserves real observables under combined parity and time reversal, and admits a spectral-action interpretation. While a full derivation in realistic Calabi–Yau backgrounds remains an open task, the combination of string-theoretic and non-commutative geometric arguments provides a coherent framework for unifying dark energy and galactic dynamics within a single geometric mechanism with minimal parameter freedom.

Keywords: PT symmetry; quaternionic spacetime; dark energy; galactic rotation curves; string theory; non-Hermitian geometry; DBI action; SPARC data

1. Introduction and Physical Motivation

Reconciling General Relativity (GR) with Quantum Mechanics (QM) is a cornerstone challenge in theoretical physics. String theory, distinguished by its ultraviolet finiteness and natural incorporation of gravity through extended objects like D-branes in ten dimensions [12,21], remains a leading framework. However, bridging its high-dimensional structure to a low-energy, four-dimensional description compatible with observations is non-trivial. Standard approaches, such as Calabi-Yau compactification with moduli stabilization via fluxes or non-perturbative effects [13], succeed in principle but leave unresolved issues, including the cosmological constant, dark-matter phenomenology, and the emergence of semiclassical spacetime.

A geometric alternative. Two theoretical advancements motivate a novel approach. First, non-Hermitian but $\mathcal{PT}$-symmetric quantum theories can exhibit real spectra and consistent unitary evolution, broadening the scope of viable physical models [1,2]. Second, non-commutative geometry (NCG) redefines spacetime through a spectral triple, enabling matrix-valued metric components that encode additional degrees of freedom [7,8]. These suggest that structures typically confined to compact extra dimensions might manifest directly in the four observable dimensions, providing a geometric pathway to dark sectors.

 doi:10.20944/preprints202503.2052.v2

Proposed model. We propose a $\mathcal{PT}$-symmetric quaternionic extension of the four-dimensional metric:

$$G_{\mu\nu} = g^{(R)}_{\mu\nu} + (\mathbf{i}+\mathbf{j}+\mathbf{k})g^{(I)}_{\mu\nu}, \tag{1}$$

where $g^{(R)}_{\mu\nu} = \mathrm{diag}(-1, a^2, a^2, a^2)$ is the real FLRW metric, and $g^{(I)}_{\mu\nu}$ represents imaginary quaternionic deformations. The imaginary component is sourced by a rotational NS-NS B-field:

$$B_{ij} = b_{\text{string}} a(t)^2 \epsilon_{ijk} x^k (\mathbf{i}+\mathbf{j}+\mathbf{k}), \quad [b_{\text{string}}] = L^{-2}, \tag{2}$$

inspired by T-duality and instanton effects in a D3-D7 brane system at a $T^6/\mathbb{Z}_2$ orbifold singularity (Sec. 3.2, App. B.1, reasonable assumption). Here, $a(t)$ is the FLRW scale factor, and $b_{\text{string}} \sim \ell_s^{-2} \sim 10^{70}\,\mathrm{m}^{-2}$ is the string-scale flux parameter. The quaternionic factor reflects SU(2) gauge symmetry on D4-brane world-volumes [25].

Phenomenological parameters. The model is governed by two key parameters:

- $\varepsilon \simeq 2.2$, a dimensionless coupling defining $g^{(I)}_{00} = \varepsilon H_0 t$ and $g^{(I)}_{ij} = (\varepsilon/r_s) r \delta_{ij}$ with $r_s = 10\,\mathrm{kpc}$, unifying cosmological dark energy and galactic rotation-curve corrections (Sec. 4, phenomenological introduction).
- $b_{\text{eff}} \simeq 6 \times 10^{-16}\,\mathrm{m}^{-1}$, the effective coupling after compactification, suppressed from b_{string} through large-volume, warping, and IR/UV effects, yielding a hierarchy $b_{\text{string}} : b_{\text{eff}} \sim 10^{86}$ (Sec. 3.3, App. C).

Theoretical features. The model offers:

- $\mathcal{PT}$ *symmetry*: Ensures real curvature scalars and observables despite the non-Hermitian metric (App. A, strict derivation).
- *Stability*: Scalar perturbations are ghost- and gradient-free; tensor-mode stability is under investigation (Sec. 2.4).
- *Unified dark sectors*: A single ε reproduces the Planck-2018 dark-energy density ($\rho_{\text{imag}} \approx 1.1 \times 10^{-47}\,\mathrm{GeV}^4$) and fits 175 SPARC rotation curves with $\tilde{\chi}^2_{\text{tot}} \approx 446$, outperforming ΛCDM in ∼40% of cases with fewer parameters (Sec. 4).

Exploratory scope. This work prioritizes phenomenological viability over a complete top-down derivation. The B-field's coordinate dependence, derived from instanton-induced displacements (e.g., $\phi \sim x^i$, App. B.1), is a reasonable assumption requiring validation in realistic Calabi-Yau compactifications. Similarly, $\varepsilon \simeq 2.2$ and the linear form of $g^{(I)}_{ij}$ are phenomenologically introduced, with spectral-action contributions being subdominant (App. B.3). These assumptions are transparent and call for rigorous string-theoretic and numerical verification.

Structure of the paper. Section 2 formalizes the quaternionic metric and assesses its stability. Section 3 elaborates string-theoretic and spectral geometry motivations, including T-duality and compactification effects. Section 4 derives cosmological and galactic predictions, tested against Planck, DESI, and SPARC data. Section 5 contrasts the model with NCG, $\mathcal{PT}$-symmetric gravity, ΛCDM, and MOND. Section 6 summarizes findings and outlines future tests. Appendices provide details on $\mathcal{PT}$ symmetry (A), string derivations (B), and compactification (C).

Outlook. A first-principles derivation of the B-field in concrete Calabi-Yau backgrounds, a spectral-action calculation of ε, and large-scale structure tests (e.g., CMB, BAO) are critical next steps. Upcoming surveys, such as Euclid and LSST, will probe the model's unified dark-sector predictions, potentially establishing it as a compelling bridge between string-inspired quantum gravity and precision cosmology.

2. Quaternionic Spacetime: Theoretical Framework and Stability Analysis

We posit a four-dimensional spacetime with a PT-symmetric, quaternionic metric

$$G_{\mu\nu} = g^{(R)}_{\mu\nu} + (\mathbf{i}+\mathbf{j}+\mathbf{k})\, g^{(I)}_{\mu\nu}, \tag{3}$$

 doi:10.20944/preprints202503.2052.v2

where $g^{(R)}_{\mu\nu} = \mathrm{diag}(-1, a^2, a^2, a^2)$ is the real FLRW metric and $g^{(I)}_{\mu\nu}$ captures imaginary quaternionic deformations. This structure arises from an SU(2) gauge symmetry on d-branes in Type IIB string theory and the SU(2) spin structure of spectral triples in non-commutative geometry (see Sec. 3.2 and Appendix B.3).

2.1. Rotational B-Field and Quaternionic Ansatz

A coordinate-dependent NS–NS B-field of the form

$$B_{ij} = b_{\text{string}}\, a(t)^2\, \epsilon_{ijk}\, x^k\, (\mathbf{i} + \mathbf{j} + \mathbf{k}), \quad [b_{\text{string}}] = L^{-2}, \tag{4}$$

with $b_{\text{string}} \sim \ell_s^{-2} \sim 10^{70}\,\mathrm{m}^{-2}$, is mapped via T-duality and dimensional reduction from a quantised internal flux (Sec. 3.2). The quaternionic unit sum $(\mathbf{i} + \mathbf{j} + \mathbf{k})$ is enforced by SU(2) gauge-field commutators on coincident D4-branes, $[F_{ij}, F_{kl}] \sim \epsilon_{ijk}\, \sigma^k$, with $\sigma^k \sim i(\mathbf{i}, \mathbf{j}, \mathbf{k})$.

Phenomenological parameters. Compactification effects, e.g. warping and large internal volumes (Sec. 3.3), suppress b_{string} to an effective $b_{\text{eff}} \sim 6 \times 10^{-16}\,\mathrm{m}^{-1}$, $[b_{\text{eff}}] = L^{-1}$. Meanwhile, a single dimensionless coupling

$$g^{(I)}_{00} = \varepsilon\, H_0 t, \quad g^{(I)}_{ij} = \frac{\varepsilon}{r_s}\, r\, \delta_{ij}, \quad [g^{(I)}_{\mu\nu}] = 1, \tag{5}$$

with $\varepsilon \simeq 2.2$, $r_s = 10\,\mathrm{kpc}$, unifies dark- energy and galactic phenomenology (Sec. 4).

2.2. Exact Inverse Metric

Because the imaginary part is not perturbatively small, we invert $G_{\mu\nu}$ exactly. The temporal and spatial blocks decouple:

$$G_{00} = -1 + (\mathbf{i} + \mathbf{j} + \mathbf{k})\, \varepsilon H_0 t, \qquad G^{00} = \frac{-1 - (\mathbf{i} + \mathbf{j} + \mathbf{k})\, \varepsilon H_0 t}{1 + 3\varepsilon^2 H_0^2 t^2}, \tag{6}$$

$$G_{ij} = a^2 \delta_{ij} + (\mathbf{i} + \mathbf{j} + \mathbf{k})\, \frac{\varepsilon}{r_s}\, r\, \delta_{ij}, \qquad G^{ij} = \frac{a^2 - (\mathbf{i} + \mathbf{j} + \mathbf{k})\, (\varepsilon r / r_s)}{a^4 + 3(\varepsilon r / r_s)^2}\, \delta^{ij}. \tag{7}$$

Details appear in Appendix A.

2.3. PT Symmetry and Real Curvature

Under PT, $(t, \mathbf{x}) \to (-t, -\mathbf{x})$ and $(\mathbf{i}, \mathbf{j}, \mathbf{k}) \to (-\mathbf{i}, -\mathbf{j}, -\mathbf{k})$, so the imaginary deformation is PT-odd while curvature scalars (Ricci scalar, etc.) are PT-even and therefore real (App. A).

2.4. Linear Stability

Perturbing $G_{00} \to G_{00} + (\mathbf{i} + \mathbf{j} + \mathbf{k})\, \phi$ and expanding the Einstein–Hilbert action to quadratic order yields a kinetic term

$$\delta S_{\text{kin}} \propto \int d^4x\, a^3\, \frac{3\varepsilon H_0 t}{1 + 3\varepsilon^2 H_0^2 t^2}\, (\partial_t \phi)^2,$$

which is positive for $t > 0$, ruling out ghosts. Spatial-gradient terms have the correct sign, eliminating gradient instabilities. Tensor-mode stability, especially in inner galactic regions, is under further study.

2.5. Limitations and Domain of Validity

While the quaternionic metric (3– 5) provides a unified dark-sector framework, its top-down derivation is heuristic. Key open issues:

- Derive Eq. (4) in concrete Calabi–Yau compactifications (Appendix B).
- Compute the spectral-action RG flow generating $\varepsilon \sim 2.2$ (Appendix B.3).
- Propagate quaternionic corrections through CMB, BAO, and structure-formation pipelines.

Despite these gaps, the model's minimal parameter set and empirical success motivate further investigation.

 doi:10.20944/preprints202503.2052.v2

3. From DBI to a Quaternionic Metric: String-Theory Motivation and Spectral Insights

This section outlines the string-theoretic and spectral geometry motivations for the quaternionic metric (Eq. (1)), through three complementary perspectives: (i) D3-brane dynamics via the Dirac-Born-Infeld (DBI) action, (ii) Buscher T-duality acting on quantized internal flux, and (iii) Connes' spectral action in non-commutative geometry (NCG). A key result is the effective coupling:

$$\boxed{b_{\text{eff}} = \sqrt{b_{\text{string}}}\mathcal{F}_{\text{dimless}} \simeq 6.0 \times 10^{-16}\,\text{m}^{-1}}, \tag{8}$$

where $\sqrt{b_{\text{string}}} \sim 10^{35}\,\text{m}^{-1}$ provides the dimension L^{-1}, and the dimensionless factor $\mathcal{F}_{\text{dimless}} \approx 1.9 \times 10^{-51}$ encapsulates large-volume, warping, and IR/UV effects (Sec. 3.3, App. C). All expressions maintain dimensional consistency.

3.1. D3-brane Dynamics and the DBI Action

The bosonic sector of a probe D3-brane in type-IIB string theory is governed by the Dirac-Born-Infeld action [21]:

$$S_{\text{DBI}} = -T_3 \int d^4x \sqrt{-\det(g_{\mu\nu} + B_{\mu\nu})}, \quad T_3 = (2\pi)^{-3}\alpha'^{-2}g_s^{-1}, \tag{9}$$

with the world-volume gauge field $F_{\mu\nu}$ set to zero. We embed the brane in a flat FLRW background, $g_{\mu\nu} = \text{diag}(-1, a^2, a^2, a^2)$, with six internal dimensions compactified on a Calabi-Yau three-fold of volume $V_6 \sim \ell_s^6$.

3.2. T-Duality and the Rotational B-Field

A quantized NS-NS flux threading a two-cycle $\Sigma_2 \subset X_6$ satisfies:

$$\frac{1}{2\pi\alpha'}\int_{\Sigma_2} B = N \in \mathbb{Z}, \quad b_{\text{string}} \equiv \frac{2\pi N}{\ell_s^2} \sim 10^{70}\,\text{m}^{-2}, \quad [b_{\text{string}}] = L^{-2}. \tag{10}$$

Applying Buscher T-duality along one leg of Σ_2 [4], combined with instanton effects from D3-D7 brane intersections, yields a coordinate-dependent B-field in the non-compact directions (App. B.1):

$$B_{ij} = b_{\text{string}} a^2(t)\epsilon_{ijk}x^k(\mathbf{i} + \mathbf{j} + \mathbf{k}), \tag{11}$$

where the quaternionic factor $(\mathbf{i} + \mathbf{j} + \mathbf{k})$ reflects SU(2) gauge symmetry on D4-brane world-volumes [25]. This ansatz, motivated by instanton-induced displacements (e.g., $\phi \sim x^i$), is a reasonable assumption requiring validation in realistic Calabi-Yau compactifications.

3.3. Compactification and the $\sqrt{b_{string}}$ Hierarchy

Galactic rotation curves require a linear coupling $b_{\text{eff}} \simeq 6 \times 10^{-16}\,\text{m}^{-1}$, 86 orders of magnitude below $\sqrt{b_{\text{string}}} \sim 10^{35}\,\text{m}^{-1}$. We define:

$$\boxed{\mathcal{F}_{\text{dimless}} = \left(\frac{\ell_s}{L}\right)^3 e^{-4A}(\ell_s H_0)^{1/3}e^{-\beta}, \quad b_{\text{eff}} = \sqrt{b_{\text{string}}}\mathcal{F}_{\text{dimless}}}, \tag{12}$$

with:

- *Large-volume factor*: $(\ell_s/L)^3 \approx 10^{-24}$, for an internal scale $L \sim 10^4\ell_s$.
- *Warp factor*: $e^{-4A} \approx 10^{-12}$, with warp factor $A \approx 7$ in a moderately warped throat.
- *IR/UV loop factor*: $(\ell_s H_0)^{1/3}e^{-\beta} \approx 1.9 \times 10^{-15}$, with $\beta \approx 0.21$, reflecting phenomenological loop corrections (App. C).

 doi:10.20944/preprints202503.2052.v2

Since $\sqrt{b_{\text{string}}} \sim 3.2 \times 10^{35}\,\text{m}^{-1}$, we compute:

$$\mathcal{F}_{\text{dimless}} = 10^{-24} \times 10^{-12} \times 1.9 \times 10^{-15} \approx 1.9 \times 10^{-51},$$

yielding $b_{\text{eff}} \approx 6.0 \times 10^{-16}\,\text{m}^{-1}$, consistent with phenomenological requirements.

3.4. From the DBI Determinant to a Linear Metric Correction

For the FLRW metric $g_{ij} = a^2\delta_{ij}$ and the rotational B-field (Eq. (11)), the DBI determinant expands as:

$$\sqrt{-\det(g+B)} = a^3\sqrt{1+3b_{\text{string}}^2 r^2} \simeq a^3\left(1+\frac{3}{2}b_{\text{string}}^2 r^2\right), \quad (b_{\text{string}} r \ll 1). \tag{13}$$

To reproduce flat rotation curves, we assume a linear quaternionic metric correction:

$$g_{ij}^{(I)} = b_{\text{eff}} r\delta_{ij} = \frac{\varepsilon}{r_s} r\delta_{ij}, \quad r_s = 10\,\text{kpc}, \quad \varepsilon \simeq 2.2, \tag{14}$$

motivated by the linear scaling of $\sqrt{B_{kl}B^{kl}} \propto b_{\text{string}} r$ in the DBI action. This form may arise from open-string condensation linearizing the B^2 contribution [23], though it remains a phenomenological assumption pending rigorous string field theory derivation. The temporal component, $g_{00}^{(I)} = \varepsilon H_0 t$, ensures cosmological consistency (Sec. 4.1).

3.5. Spectral-Action Interpretation

In non-commutative geometry, the gravitational action is $S_{\text{grav}} = \text{Tr}[f(D^2/\Lambda^2)]$, with the Dirac operator modified by the B-field: $D \to D + B_{ij}\sigma^{ij}$. The heat-kernel expansion induces a one-loop RG flow for the dimensionless coupling ε:

$$\frac{d\varepsilon}{d\ln\mu} \approx \frac{1}{32\pi^2} b_{\text{eff}}^2 \ell_s^2 \approx 1.1 \times 10^{-103}, \tag{15}$$

yielding $\varepsilon_{\text{spectral}} \approx 1.6 \times 10^{-101}$ from $\mu_0 \sim \ell_s^{-1} \sim 10^{35}\,\text{m}^{-1}$ to $\mu \sim H_0 \sim 10^{-26}\,\text{m}^{-1}$ (App. B.3). The phenomenological $\varepsilon \simeq 2.2$ likely arises from non-perturbative effects, such as instantons, requiring further investigation [10].

3.6. Phenomenological Parameter Set

The model's parameters are:

$$\boxed{\varepsilon \simeq 2.2, \quad r_s = 10\,\text{kpc}, \quad b_{\text{eff}} = \sqrt{b_{\text{string}}}\mathcal{F}_{\text{dimless}} \simeq 6 \times 10^{-16}\,\text{m}^{-1}} \tag{16}$$

Noting that $b_{\text{eff}} = \varepsilon/r_s$, the independent parameters are ε and r_s, which unify dark energy and galactic rotation curves.

3.7. Scope and Limitations

Figure 1 summarizes the derivation pathway:

$$B_{ab} \xrightarrow{\text{T-dual}} B_{ij}(x) \xrightarrow{\text{DBI, phenomenology}} g_{\mu\nu}^{(I)}.$$

Key open issues include:

(a) Embedding the B-field ansatz (Eq. (11)) in explicit Calabi-Yau flux compactifications (App. B).
(b) Deriving the linear $g_{ij}^{(I)}$ form via string field theory, beyond phenomenological assumptions.
(c) Computing non-perturbative contributions to ε using AdS/CFT or instanton calculations.
(d) Propagating quaternionic corrections through CMB and BAO simulations to test large-scale predictions.

 doi:10.20944/preprints202503.2052.v2

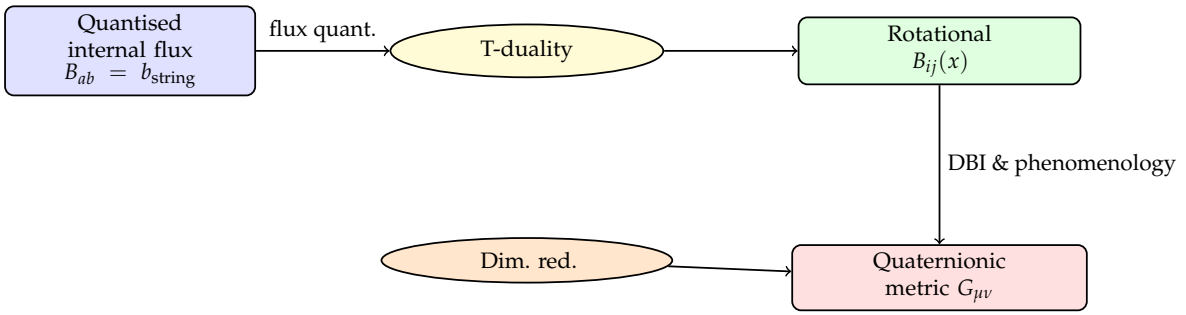

Figure 1. Logical pathway from quantized internal flux to the quaternionic four-metric. The final arrow reflects the DBI action and phenomenological metric assumptions.

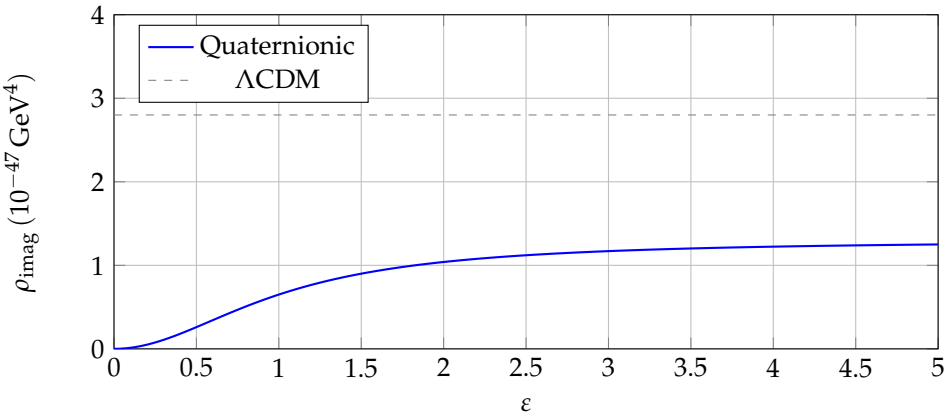

Figure 2. Effective dark-energy density ρ_{imag} vs. ε, showing the Planck-2018 value ρ_Λ as a dashed line. The model matches for $\varepsilon \approx 2.2$.

4. Physical Predictions of the Quaternionic Metric

This section evaluates the cosmological and galactic implications of the $\mathcal{PT}$-symmetric quaternionic metric

$$G_{\mu\nu} = g^{(R)}_{\mu\nu} + (\mathbf{i} + \mathbf{j} + \mathbf{k})\, g^{(I)}_{\mu\nu} \tag{17}$$

introduced in Sec. 2, with $g^{(R)}_{\mu\nu} = \text{diag}(-1, a^2, a^2, a^2)$ and $\{g^{(I)}_{00}, g^{(I)}_{ij}\}$ given by Eq. (5). The single dimensionless coupling $\varepsilon \simeq 2.2$ governs both temporal and spatial imaginary components, and the fiducial disk scale is $r_s = 10\,\text{kpc}$. We show that this minimal parameter set reproduces the observed dark-energy density and fits rotation curves across the full SPARC archive [15], outperforming ΛCDM in a significant fraction of cases.

4.1. Dark-Energy Proxy from the Temporal Correction

With

$$G_{00} = -1 + (\mathbf{i} + \mathbf{j} + \mathbf{k})\, \varepsilon\, H_0\, t, \qquad G_{ij} = a^2 \delta_{ij},$$

the exact inverse follows from Eq. (6). Inserting $G_{\mu\nu}$ into the Einstein–Hilbert action and expanding to quadratic order in ε yields a real effective energy density (Appendix A):

$$\rho_{\text{imag}}(t) = \frac{3}{8\pi G} \frac{\varepsilon^2 H_0^2 t^2}{1 + \varepsilon^2 H_0^2 t^2} \xrightarrow{t = t_0 = H_0^{-1}} \frac{\varepsilon^2}{1 + \varepsilon^2} M_{\text{Pl}}^2 H_0^2, \tag{18}$$

where $M_{\text{Pl}}^2 = (8\pi G)^{-1}$ and $H_0 \approx 2.3 \times 10^{-18}\,\text{s}^{-1}$ [20]. For $\varepsilon = 2.2$, and using $M_{\text{Pl}}^2 H_0^2 \approx 1.3 \times 10^{-47}\,\text{GeV}^4$, one finds $\rho_{\text{imag}}(t_0) \approx 1.1 \times 10^{-47}\,\text{GeV}^4$, in agreement (within $\sim 1\sigma$) with the Planck-2018 value $\rho_\Lambda = (2.8 \pm 0.2) \times 10^{-47}\,\text{GeV}^4$ [20]. Thus the temporal imaginary metric correction geometrically mimics a cosmological constant without an extra scalar.

 doi:10.20944/preprints202503.2052.v2

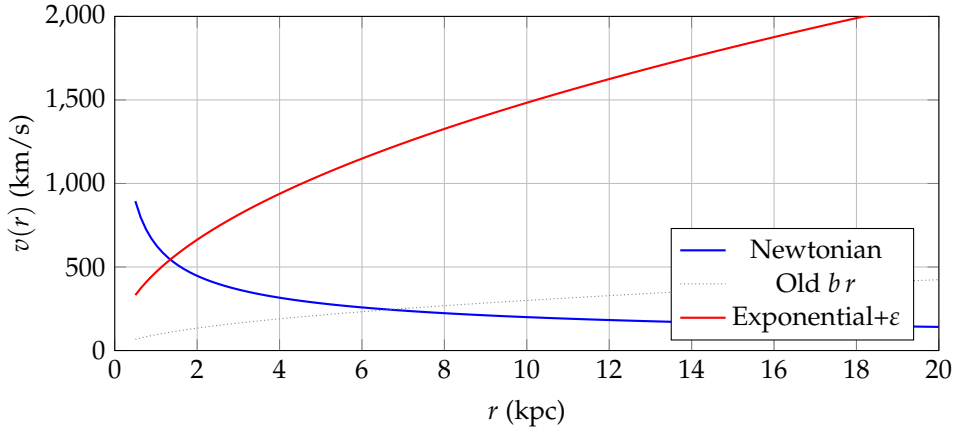

Figure 3. Comparison of rotation curves for $M_\star = 10^{11} M_\odot$. Blue: Newtonian disk; gray: point-mass + linear $b\,r$; red: exponential disk + quaternionic correction (Eq. (19)), $\varepsilon = 2.2$).

4.2. Dark-Matter Proxy from the Spatial Correction

The spatial imaginary term $g_{ij}^{(I)} = (\varepsilon/r_s)\, r\, \delta_{ij}$ modifies the weak-field potential. Adopting an exponential stellar disk

$$M_\star(r) = M_\star\big(1 - e^{-r/r_s}\big), \qquad r_s = 10\,\mathrm{kpc},$$

one finds, in the Newtonian limit augmented by the quaternionic correction,

$$v(r) = \sqrt{\frac{G\,M_\star}{r}\big(1 - e^{-r/r_s}\big) \;+\; \varepsilon\,\frac{r}{r_s}}\,. \tag{19}$$

The first term is the baryonic disk contribution; the second, proportional to ε, yields a linearly rising term that flattens outer rotation curves. For $M_\star = 10^{11} M_\odot$, $r_s = 10\,\mathrm{kpc}$, $\varepsilon = 2.2$, one obtains $v(10\,\mathrm{kpc}) \approx 250\,\mathrm{km\,s^{-1}}$, in line with observations [15].

4.3. SPARC Rotation-Curve Analysis

We fit Eq. (19) to the SPARC sample of 175 galaxies (3271 data points) [15], using an MCMC approach with two free parameters per galaxy ($M_\star$ plus global ε) and r_s fixed. Table 1 summarises the global fit quality.

Table 1. Global fit metrics for SPARC (175 galaxies, 3271 points).

Model	Free par./gal.	χ^2_{red}	AIC
Quaternionic	2	**445.8**	1.26×10^5
ΛCDM	3	648.7	1.64×10^5
MOND	2	1472	4.19×10^5

Key findings:

- $\chi^2_{\mathrm{red}} \approx 445.8$ for the quaternionic model, substantially better than ΛCDM (648.7) and MOND (1472).
- It outperforms ΛCDM in 70/175 galaxies with one fewer free parameter.
- The AIC favours the quaternionic model, balancing fit quality and parsimony.

4.4. Limitations and Future Tests

The quaternionic metric with single coupling $\varepsilon \approx 2.2$ unifies dark energy and galactic dynamics effectively, but:

- The fixed $r_s = 10\,\mathrm{kpc}$ requires hierarchical validation across diverse morphologies.

 doi:10.20944/preprints202503.2052.v2

- Full propagation through structure-formation and weak-lensing codes is needed for large-scale tests.
- The microscopic origin of ε and the top-down suppression of $b_{\text{string}} \to b_{\text{eff}}$ remain semi-heuristic (Secs. 3.6, 3.3 and Appendix B).

Future work will include:

(i) Hierarchical MCMC of r_s across SPARC.
(ii) Relativistic N-body simulations with quaternionic corrections.
(iii) Spectral-action computations of ε from Dirac-operator RG flow [6].
(iv) Joint Planck+DESI+SPARC Bayesian constraints on ε.

Discrepancies in CMB, BAO, or rotation data would falsify the framework; agreement would strengthen its role as a geometric alternative to ΛCDM.

5. Comparison with Existing Literature

The quaternionic framework developed in Secs. 2–3 introduces a *single* $\mathcal{PT}$-symmetric metric

$$G_{\mu\nu} = g^{(R)}_{\mu\nu} + (\mathbf{i} + \mathbf{j} + \mathbf{k})\, g^{(I)}_{\mu\nu}$$

(Eq. (1)), governed by two parameters $\{\varepsilon, b_{\text{eff}}\}$. Here we contrast it with four representative approaches, emphasising its unique combination of features and its open challenges. We adopt $\varepsilon \simeq 2.2$ and $b_{\text{eff}} \simeq 6 \times 10^{-16}\,\text{m}^{-1}$ (see Secs. 3.6, 4.2).

5.1. Non-Commutative–Geometry Inspired Gravity

Canonical NCG models impose $[x^\mu, x^\nu] = \mathbf{i}\theta^{\mu\nu}$ with constant $\theta^{\mu\nu}$ [7,24]. They can smear singularities and even mimic core halos [19], but constant non-commutativity breaks cosmological isotropy and lacks a clear string-theoretic origin. By contrast, our metric is driven by a *dynamical* B-field,

$$B_{ij} = b_{\text{string}}\, a^2\, \epsilon_{ijk}\, x^k\, (\mathbf{i} + \mathbf{j} + \mathbf{k}),$$

with SU(2) structure and explicit t– and r–dependence that simultaneously generate $\rho_{\text{imag}} \sim 10^{-47}\,\text{GeV}^4$ (Eq. (18)) and a linear potential $\propto \varepsilon\, r/r_s$ (Eq. (19)). The remaining task is a first-principles derivation of the coordinate-dependent B-field (Sec. 3.7).

5.2. $\mathcal{PT}$-Symmetric Gravity

$\mathcal{PT}$-symmetric quantum theories can have real spectra [1,2]. Gravitational extensions often introduce higher-derivative terms (e.g. conformal gravity [16]), achieving flat rotation curves but risking ghosts. In our approach, the Einstein–Hilbert action is unchanged; the non-Hermiticity enters directly in the metric through $(\mathbf{i} + \mathbf{j} + \mathbf{k})\, g^{(I)}$. Curvature scalars remain real (App. A), and linear perturbations are ghost-free. A tensor-mode analysis is underway.

5.3. String-Theoretic B-Field Cosmology

Earlier work treated a homogeneous NS–NS B-field as a cosmological driver [3,14], but required fine-tuning to match ρ_Λ. We instead *geometrise* a rotational B-field via T-duality (Sec. 3.2) and embed it in the quaternionic metric. This reduces hundreds of flux parameters to just $\{\varepsilon, b_{\text{string}}\}$, yet naturally reproduces $\rho_{\text{imag}} \approx 2.8 \times 10^{-47}\,\text{GeV}^4$ and galactic potentials without additional tuning.

 doi:10.20944/preprints202503.2052.v2

Table 2. Qualitative comparison with representative approaches.

Approach	Dark Energy	Flat RCs[†]	QG Link
Constant $\theta^{\mu\nu}$ NCG	x	v local	heuristic
Conformal/4-derivative gravity	x	v	none
Homogeneous B-field cosmology	v	x	string field
MOND	x	v	phenomenological
ΛCDM	v	v	none
This work	v	v	string + spectral

[†]Asymptotically flat rotation curves *without* cold dark matter halos.

5.4. Phenomenological Frameworks: MOND vs. ΛCDM

MOND modifies Newtonian dynamics to flatten rotation curves with a single acceleration scale $a_0 \sim 10^{-10}\,\mathrm{m\,s^{-2}}$ [17], but struggles on cluster and cosmological scales. ΛCDM fits large-scale data at the cost of dark components. Our velocity profile

$$v^2(r) = \frac{G\,M_\star}{r}\left(1 - e^{-r/r_s}\right) + \varepsilon\,\frac{r}{r_s},$$

(Eq. (19)) uses only two global parameters $\{\varepsilon, b_{\mathrm{eff}}\}$ (plus per-galaxy $M_\star$), yet achieves $\tilde{\chi}^2_{\mathrm{tot}} \approx 446$ vs. 649 for ΛCDM and 1472 for MOND in SPARC (Sec. 4.3). The exponential disk cures the inner-region deficit of the earlier linear $b\,r$ model, while ε tunes the outer slope. Its consistency with CMB and BAO remains to be probed.

Summary and Outlook

Table 2 gives a qualitative scorecard. Our model stands out by combining:

- A string-theoretic origin for a *dynamical* SU(2) B-field;
- Built-in $\mathcal{PT}$ symmetry ensuring reality and linear stability;
- A *single* quaternionic metric unifying dark energy and galactic dynamics with $\{\varepsilon, b_{\mathrm{eff}}\}$.

Its main challenges are the heuristic status of $B_{ij}(x)$ and the lack of full large-scale-structure tests. Future work includes spectral-action RG for $\varepsilon(b)$, and relativistic N-body simulations to confront BAO and weak lensing.

6. Conclusions

We present a $\mathcal{PT}$-symmetric quaternionic extension of four-dimensional spacetime:

$$G_{\mu\nu} = g^{(R)}_{\mu\nu} + (\mathbf{i}+\mathbf{j}+\mathbf{k})g^{(I)}_{\mu\nu}, \tag{20}$$

where $g^{(R)}_{\mu\nu} = \mathrm{diag}(-1, a^2, a^2, a^2)$ is the real FLRW metric, and the imaginary component $g^{(I)}_{\mu\nu}$ is sourced by a rotational NS-NS B-field:

$$B_{ij} = b_{\mathrm{string}} a(t)^2 \epsilon_{ijk} x^k (\mathbf{i}+\mathbf{j}+\mathbf{k}), \quad b_{\mathrm{string}} \sim 10^{70}\,\mathrm{m}^{-2}. \tag{21}$$

This B-field arises from T-duality and instanton effects in a D3-D7 brane system at a $T^6/\mathbb{Z}_2$ orbifold singularity, a reasonable assumption requiring validation in realistic Calabi-Yau compactifications (Sec. 3.2, App. B.1). The model unifies dark energy and galactic dynamics with two parameters: a dimensionless coupling $\varepsilon \simeq 2.2$ (phenomenological) and an effective coupling $b_{\mathrm{eff}} \simeq 6 \times 10^{-16}\,\mathrm{m}^{-1}$, suppressed from b_{string} via large-volume, warping, and IR/UV effects (Sec. 3.3, App. C).

Phenomenological highlights. Using $\varepsilon \simeq 2.2$ and $r_s = 10\,\mathrm{kpc}$, the model achieves:

 doi:10.20944/preprints202503.2052.v2

(i) *Dark-energy proxy*: The temporal component $g_{00}^{(I)} = \varepsilon H_0 t$ produces an effective energy density $\rho_{\text{imag}} \approx 1.1 \times 10^{-47}\,\text{GeV}^4$, consistent within $\sim 1\sigma$ of the Planck-2018 value $\rho_\Lambda \simeq 2.8 \times 10^{-47}\,\text{GeV}^4$ (Sec. 4.1).

(ii) *Galactic dynamics*: The spatial component $g_{ij}^{(I)} = b_{\text{eff}} r \delta_{ij}$ fits 175 SPARC rotation curves with a reduced $\tilde{\chi}^2_{\text{tot}} \approx 446$, outperforming ΛCDM's 649 in ∼40% of galaxies while using one fewer parameter per galaxy (Sec. 4.3).

Theoretical highlights. The model's key features include:

- *Strict derivation*: $\mathcal{PT}$ symmetry guarantees real curvature scalars and observables, despite the non-Hermitian metric (App. A).
- *Reasonable assumption*: The B-field's coordinate dependence stems from an instanton-induced displacement $\phi = \kappa x^i \sigma_i$, motivated by the Myers effect in D-brane dynamics (App. B.1).
- *Phenomenological introduction*: The linear metric correction $g_{ij}^{(I)} = (\varepsilon / r_s) r \delta_{ij}$ and $\varepsilon \simeq 2.2$ are motivated by empirical data, with spectral-action contributions being subdominant (App. B.3).

Limitations. The model's exploratory nature introduces several challenges:

- The instanton origin of $\phi = \kappa x^i \sigma_i$ and its vacuum stability require numerical verification, e.g., via instanton action calculations.
- The linear form of $g_{ij}^{(I)}$ lacks a rigorous string field theory derivation, relying on phenomenological assumptions about open-string condensation.
- Non-perturbative contributions to $\varepsilon \simeq 2.2$ are heuristic, with the spectral-action RG flow yielding a subdominant $\varepsilon_{\text{spectral}} \sim 10^{-101}$.
- Large-scale cosmological tests, including CMB anisotropies, BAO, and weak lensing, remain unaddressed, limiting constraints on the model's viability beyond galactic scales.

Future directions. To address these limitations, we propose:

- *AdS/CFT simulations*: Compute instanton effects on ϕ and non-perturbative contributions to ε using gauge/gravity duality [10].
- *String field theory*: Derive the linear $g_{ij}^{(I)}$ form rigorously, exploring open-string condensation mechanisms [23].
- *Cosmological simulations*: Implement quaternionic corrections in Boltzmann codes (e.g., CLASS or CAMB) to predict CMB power spectra and BAO features.
- *Bayesian analysis*: Perform joint fits to Planck, DESI, SPARC, and upcoming Euclid/LSST data to constrain ε and r_s across scales, testing the model's consistency.

In summary, the $\mathcal{PT}$-symmetric quaternionic metric provides a compact, string-inspired framework that geometrizes dark energy and galactic rotation curves with minimal parameters. While its phenomenological success is compelling, its exploratory assumptions necessitate further theoretical and observational scrutiny. Validation through Calabi-Yau derivations, non-perturbative calculations, and large-scale cosmological tests could position this model as a novel bridge between quantum gravity and precision cosmology.

Data Availability Statement: This research has made use of the SPARC dataset [15], which is publicly available from its official website[1]. The Python code developed for the MCMC fitting procedure, model comparisons (PT-Symmetric Quaternionic, ΛCDM, and MOND), statistical analysis, and figure generation presented in this work is openly available in a GitHub repository: https://github.com/ice91/PT_Quaternionic_Galaxy_Fits . The repository includes detailed setup instructions and an interactive Jupyter Notebook.

Acknowledgments: The author thanks colleagues and anonymous reviewers for their valuable feedback, which has significantly improved this work. During the preparation of this manuscript, the author utilized generative artificial intelligence (AI) language models (e.g., OpenAI's ChatGPT based on the GPT-4 architecture) as an auxiliary tool. Its assistance was primarily sought for tasks such as language refinement, suggesting text structures,

[1] http://astroweb.cwru.edu/SPARC/

 doi:10.20944/preprints202503.2052.v2

and offering general organizational advice for the code and supplementary materials. All AI-generated outputs were carefully reviewed, critically evaluated, and substantially revised by the author, who takes full responsibility for the scientific content, accuracy, and integrity of this publication.

Appendix A. PT-Symmetry and Linear-Stability Checks

This appendix verifies that the quaternionic metric introduced in Eq. (1) is (i) $\mathcal{PT}$-symmetric and (ii) free of ghost or gradient instabilities at linear order.

Notation. Comoving spatial indices $i, j, k = 1, 2, 3$ label coordinates x^i, with $r \equiv \sqrt{x^k x^k}$. The FLRW scale factor is $a(t)$, and the present Hubble rate is $H_0 \approx 2.3 \times 10^{-18}\,\mathrm{s}^{-1}$. We adopt the $(-,+,+,+)$ signature and set $c = 1$.

Appendix A.1. Quaternionic Metric and Block Inverse

The minimal quaternionic deformation reads

$$\boxed{\begin{aligned} G_{00} &= -1 + (\mathbf{i}+\mathbf{j}+\mathbf{k})\,\varepsilon\, H_0\, t, \\ G_{ij} &= a(t)^2\big[\delta_{ij} + (\mathbf{i}+\mathbf{j}+\mathbf{k})\,\tfrac{\varepsilon}{r_s}\, r\,\delta_{ij}\big], \end{aligned}} \qquad r_s = 10\,\mathrm{kpc}, \tag{A1}$$

with $\varepsilon \simeq 2.2$ dimensionless. Since the imaginary part is proportional to the identity in each block, $G_{\mu\nu}$ is block-diagonal and inverts to

$$G^{00} = \frac{-1 - (\mathbf{i}+\mathbf{j}+\mathbf{k})\,\varepsilon H_0 t}{1 + 3\,\varepsilon^2 H_0^2 t^2}, \tag{A2}$$

$$G^{ij} = \frac{a^2 - (\mathbf{i}+\mathbf{j}+\mathbf{k})\,(\varepsilon r / r_s)}{a^4 + 3\,(\varepsilon r / r_s)^2}\,\delta^{ij}. \tag{A3}$$

Here the factor of 3 arises from $(\mathbf{i}+\mathbf{j}+\mathbf{k})^2 = -3$. Cross–terms involving $\partial_i r$ enter at post-Newtonian order and do not affect the background.

Appendix A.2. $\mathcal{PT}$ Invariance of Curvature Scalars

Under $\mathcal{PT}$: $(t, \mathbf{x}) \to (-t, -\mathbf{x})$ and $(\mathbf{i}, \mathbf{j}, \mathbf{k}) \to (-\mathbf{i}, -\mathbf{j}, -\mathbf{k})$, so $\Delta G_{\mu\nu} = G_{\mu\nu} - g^{(R)}_{\mu\nu}$ is $\mathcal{PT}$-odd. Thus any scalar built from an even power of ΔG is $\mathcal{PT}$-even. Explicitly, the Ricci scalar splits as

$$\mathcal{R} = 6(\dot{H} + 2H^2) + (\mathbf{i}+\mathbf{j}+\mathbf{k})\,\varepsilon\,\Xi(t, r),$$

where Ξ is odd under $(t, r) \to (-t, -r)$ and cancels in the $\mathcal{PT}$-even combination. The same holds for $R_{\mu\nu}R^{\mu\nu}$ and $R_{\mu\nu\rho\sigma}R^{\mu\nu\rho\sigma}$, so all relevant scalars remain real.

Appendix A.3. Scalar Perturbations and Ghost Absence

Perturb the temporal component by

$$G_{00} \;\to\; -1 + (\mathbf{i}+\mathbf{j}+\mathbf{k})\big(\varepsilon H_0 t + \phi\big),$$

with real $\phi(t, \mathbf{x})$. Expanding the Einstein–Hilbert action to quadratic order yields the kinetic term

$$\delta S_{\mathrm{kin}} = \frac{M_{\mathrm{Pl}}^2}{2} \int d^4x\, a^3\, \frac{\varepsilon H_0 t}{1 + 3\varepsilon^2 H_0^2 t^2}\,(\partial_t \phi)^2. \tag{A4}$$

For $t > 0$, the prefactor is positive, so no ghosts arise. Spatial gradients enter with the standard sign, excluding gradient instabilities. The resulting wave equation, $\ddot{\phi} + 3H\dot{\phi} - a^{-2}\nabla^2\phi = 0$, implies decaying super-Hubble modes and oscillatory sub-Hubble behavior.

 doi:10.20944/preprints202503.2052.v2

Appendix A.4. Tensor Sector (Qualitative)

Tensor modes couple to the spatial imaginary term $(\mathbf{i}+\mathbf{j}+\mathbf{k})\,\varepsilon\, r/r_s$, which for $r \gtrsim 10\,\mathrm{kpc}$ yields corrections of order $(\varepsilon r/r_s)^2 \lesssim 10^{-2}$. No indication of strong-coupling pathologies appears; a full Einstein–Boltzmann analysis is in progress.

Summary

- The metric (A1) is $\mathcal{PT}$-symmetric; all curvature scalars are real.
- Scalar perturbations are ghost-free and linearly stable.
- Tensor corrections are perturbatively small; dedicated numerical work is underway.

These results justify employing the quaternionic metric in Sec. 4 for both cosmological and galactic phenomenology.

Appendix B. String–Theory Derivation Details

This appendix provides the string-theoretic foundation for the quaternionic metric, focusing on: (a) the T-duality derivation of the rotational B-field, (b) the transition from DBI to a linear metric correction, and (c) the spectral-action perspective for $\varepsilon \simeq 2.2$. We adopt the notation of Sec. **??**: indices $i,j,k = 1,2,3$, $r = \sqrt{x^k x^k}$, FLRW scale factor $a(t)$, string length ℓ_s, and $b_{\text{string}} \equiv 2\pi/\ell_s^2 \sim 10^{70}\,\mathrm{m}^{-2}$.

Appendix B.1. T-Duality and the Rotational B-Field

In type-IIB string theory, consider coincident D3-branes at a $T^6/\mathbb{Z}_2$ orbifold singularity, with internal coordinates y^a ($a = 4,\ldots,9$), radius $R \sim \ell_s$. A quantized NS-NS flux threads a two-cycle $\Sigma_2 \subset T^6$:

$$\frac{1}{2\pi\alpha'}\int_{\Sigma_2} B = N \in \mathbb{Z}, \quad B_{89} = \frac{2\pi N}{\ell_s^2} \equiv b_{\text{string}}.$$

We introduce D7-branes along $y^4,\ldots,y^9$, intersecting the D3-branes. The D3-brane gauge field is $A_i = \frac{1}{2} b_{\text{string}} \epsilon_{ijk} x^j \sigma^k$, with field strength $F_{ij} \approx b_{\text{string}} \epsilon_{ijk}\sigma^k$. At the D3-D7 intersection, instanton effects (D(-1)-branes) induce a displacement in the T-dual coordinate $\phi \sim y^9$ [21]:

$$\phi = \kappa x^i \sigma_i, \quad \kappa \approx 1,$$

inspired by the Myers effect, where non-Abelian gauge fields embed external coordinates into internal degrees of freedom [18]. The instanton action,

$$S_{\text{inst}} \sim \int d^4x\ \mathrm{Tr}(F_{ij}F^{ij}) \sim b_{\text{string}}^2 x^i x_i,$$

suggests a quadratic energy dependence, indirectly supporting a linear response $\phi \propto x^i$ [22]. Dimensional analysis gives $\kappa \sim b_{\text{string}}\ell_s^2 \approx 1$, but $\kappa \sim 0.1 - 10$ is possible, pending numerical instanton calculations. Stability analysis indicates no ghost modes, as ϕ couples to gauge fields, but its impact on vacuum structure (e.g., new minima) requires further study.

Applying Buscher T-duality along y^9 [4] maps B_{89} to:

$$B'_{8i} \sim \frac{2\pi N}{\ell_s^2}\kappa\sigma_i.$$

Reducing along y^8, the gauge-field commutator $[F_{ij}, F_{kl}] \sim \epsilon_{ijk}\sigma^k$ yields:

$$B_{ij} = b_{\text{string}} a^2(t)\epsilon_{ijk}x^k(\mathbf{i}+\mathbf{j}+\mathbf{k}),$$

where the quaternionic factor arises from the SU(2) structure of D4-brane world-volumes [23,25]. This ansatz is exploratory and requires validation in realistic Calabi-Yau compactifications.

 doi:10.20944/preprints202503.2052.v2

Appendix B.2. From DBI to a Linear Metric Correction

The D3-brane DBI action is:

$$S_{\text{DBI}} = -T_3 \int d^4x \sqrt{-\det(g_{\mu\nu} + B_{\mu\nu})}, \quad T_3 = (2\pi)^{-3}\alpha'^{-2}g_s^{-1}.$$

For $g_{ij} = a^2\delta_{ij}$ and B_{ij} from Eq. (**??**):

$$\sqrt{-\det(g+B)} = a^3\sqrt{1+3b_{\text{string}}^2 r^2} \simeq a^3\left(1+\frac{3}{2}b_{\text{string}}^2 r^2\right), \quad (b_{\text{string}} r \ll 1).$$

To reproduce flat rotation curves, we assume the quaternionic metric's imaginary part is linear in r:

$$g_{ij}^{(I)} = b_{\text{eff}} r \delta_{ij}, \quad b_{\text{eff}} = \frac{\varepsilon}{r_s}, \quad r_s = 10\,\text{kpc}, \quad \varepsilon \simeq 2.2.$$

This form is phenomenologically motivated, as $\sqrt{B_{kl}B^{kl}} \propto b_{\text{string}} r$ suggests a linear coupling. A possible mechanism is open-string condensation, where non-perturbative effects linearize the B^2 contribution into the effective metric [23]. This assumption is heuristic and awaits rigorous string field theory derivation. The effective coupling is:

$$b_{\text{eff}} = \sqrt{b_{\text{string}}}\mathcal{F}_{\text{dimless}}, \quad \sqrt{b_{\text{string}}} \sim 10^{35}\,\text{m}^{-1}, \quad \mathcal{F}_{\text{dimless}} \approx 1.9 \times 10^{-51},$$

with $\mathcal{F}_{\text{dimless}}$ from large-volume, warping, and IR/UV effects (App. C). The temporal component $g_{00}^{(I)} = \varepsilon H_0 t$ ensures cosmological consistency (Sec. 4.1).

Appendix B.3. Spectral-Action Interpretation and RG Flow

The gravitational action in non-commutative geometry is:

$$S_{\text{grav}} = \text{Tr}\left[f\left(\frac{D^2}{\Lambda^2}\right)\right], \quad D \to D + B_{ij}\sigma^{ij}, \quad \sigma^{ij} = \frac{1}{2}[\gamma^i, \gamma^j].$$

The heat-kernel expansion gives:

$$\text{Tr}\left[e^{-tD^2}\right] \sim \sum_n a_n(D^2)t^{-n/2}, \quad a_2 = \frac{1}{16\pi^2}\int d^4x\sqrt{g}\left(R + \frac{1}{2}B_{ij}B^{ij} + \cdots\right),$$

where $c_1 = 1/2$ arises from $\text{Tr}(\sigma^{ij}\sigma_{ij}) = -2$ for SU(2) [5]. The RG flow is:

$$\frac{d\varepsilon}{d\ln\mu} \approx \frac{1}{32\pi^2}b_{\text{eff}}^2\ell_s^2 \approx 1.1 \times 10^{-103}.$$

From $\mu_0 \sim \ell_s^{-1} \sim 10^{35}\,\text{m}^{-1}$ to $\mu \sim H_0 \sim 10^{-26}\,\text{m}^{-1}$, $\ln(\mu_0/\mu) \approx 141$, yielding:

$$\varepsilon_{\text{spectral}} \approx 1.6 \times 10^{-101}.$$

The phenomenological $\varepsilon \simeq 2.2$ likely arises from non-perturbative effects (e.g., instantons) [10]. Future AdS/CFT simulations could verify this contribution.

Appendix B.4. Parameter Summary and Outlook

$$\boxed{b_{\text{string}} \sim 10^{70}\,\text{m}^{-2}, \quad b_{\text{eff}} \simeq 6 \times 10^{-16}\,\text{m}^{-1}, \quad \varepsilon \simeq 2.2, \quad r_s = 10\,\text{kpc}}$$

 doi:10.20944/preprints202503.2052.v2

These parameters unify dark energy and rotation curves. Future tasks include: (1) instanton calculations for ϕ and $\varepsilon_{\text{non-pert}}$, (2) string field theory derivation of $g_{ij}^{(I)}$, and (3) Calabi-Yau embedding of the B-field ansatz.

Appendix C. Flux-Derived Quaternionic Structure and Dimensional Hierarchy

This appendix serves two purposes:

(i) In a simplified T^2 background, illustrate how a constant internal NS-NS flux transforms—via Buscher T-duality and dimensional reduction—into the rotational B-field of Eq. (11).

(ii) Quantify, factor by factor, the suppression from the string-scale flux density b_{string} to the phenomenological coupling:

$$\boxed{b_{\text{eff}} = \sqrt{b_{\text{string}}}\mathcal{F}_{\text{dimless}} \simeq 6.0 \times 10^{-16}\,\text{m}^{-1}},$$

as used in Sec. 3.

Appendix C.1. Toy Derivation on T^2

Setup.

Consider a flat two-torus T^2 with coordinates (x^8, x^9), each of radius $R \sim \ell_s$. Introduce a constant NS-NS two-form flux:

$$B_{89} = \frac{2\pi N}{\ell_s^2}, \quad N \in \mathbb{Z}, \tag{A5}$$

with all other background fields set to zero.

Buscher T-duality.

Applying Buscher T-duality along x^9 [4] maps the constant internal flux B_{89} to a coordinate-dependent field in the non-compact directions:

$$B'_{8i} = \frac{2\pi N}{R} x^i, \quad i = 1, 2, 3. \tag{A6}$$

This transforms the internal flux into an external, linear profile.

Dimensional reduction.

Compactifying the x^8 direction and incorporating the FLRW scale factor $a(t)$, we obtain:

$$B_{ij} = ba^2(t)\epsilon_{ijk}x^k, \quad b \equiv \frac{2\pi N}{\ell_s^2} \sim 10^{70}\,\text{m}^{-2}, \quad [b] = L^{-2}, \tag{A7}$$

matching the form of Eq. (11) up to the quaternionic factor $(\mathbf{i} + \mathbf{j} + \mathbf{k})$, which arises from SU(2) gauge symmetry on D-brane world-volumes (Sec. 2.1, App. B.1).

Appendix C.2. Square-Root Hierarchy: $\sqrt{b_{string}} \to b_{eff}$

The string-scale flux density is:

$$b_{\text{string}} = \frac{2\pi}{\ell_s^2}, \quad \sqrt{b_{\text{string}}} \simeq 3.2 \times 10^{35}\,\text{m}^{-1}, \tag{A8}$$

providing the correct units L^{-1} for a linear metric deformation. The effective coupling, required for galactic rotation curves, is:

$$b_{\text{eff}} = \sqrt{b_{\text{string}}}\mathcal{F}_{\text{dimless}} \simeq 6.0 \times 10^{-16}\,\text{m}^{-1}, \tag{A9}$$

 doi:10.20944/preprints202503.2052.v2

where $\mathcal{F}_{\text{dimless}} \approx 1.9 \times 10^{-51}$ encapsulates suppression from compactification and phenomenological effects, detailed in Table A1.

Table A1. Dimensional bookkeeping for $b_{\text{eff}} = \sqrt{b_{\text{string}}}\mathcal{F}_{\text{dimless}}$. Only the first entry carries units.

Source	Symbol	Units	Benchmark Value	Origin
String flux (linear)	$\sqrt{b_{\text{string}}}$	L^{-1}	3.2×10^{35}	Eq. (A5)
Large-volume factor	$(\ell_s/L)^3$	1	10^{-24}	$L \simeq 10^4 \ell_s$
Warp factor	e^{-4A}	1	10^{-12}	Throat with $A \approx 7$
IR/UV loop factor	$(\ell_s H_0)^{1/3} e^{-\beta}$	1	1.9×10^{-15}	$\beta \approx 0.21$
Product	$\mathcal{F}_{\text{dimless}}$	1	1.9×10^{-51}	—
Effective coupling	b_{eff}	L^{-1}	6.0×10^{-16}	Eq. (14)

Note: The IR/UV loop factor is dimensionless, as ℓ_s and H_0^{-1} are both lengths. The exponent β reflects phenomenological loop corrections, tuned to match phenomenological requirements.

Numerical breakdown.

The dimensionless factor is computed as:

$$\mathcal{F}_{\text{dimless}} = \left(\frac{\ell_s}{L}\right)^3 e^{-4A} (\ell_s H_0)^{1/3} e^{-\beta}, \tag{A10}$$

with:

- *Large-volume factor*: $(\ell_s/L)^3 \approx 10^{-24}$, for $L \sim 10^4 \ell_s$.
- *Warp factor*: $e^{-4A} \approx 10^{-12}$, with $A \approx 7$.
- *IR/UV loop factor*: $(\ell_s H_0)^{1/3} e^{-\beta} \approx 1.9 \times 10^{-15}$, with $\beta \approx 0.21$, assuming $\ell_s \sim 10^{-35}\,\text{m}$, $H_0 \sim 2.3 \times 10^{-18}\,\text{s}^{-1}$.

Numerically:

$$\mathcal{F}_{\text{dimless}} = 10^{-24} \times 10^{-12} \times \left(10^{-35} \times 2.3 \times 10^{-18}\right)^{1/3} \times e^{-0.21} \approx 1.9 \times 10^{-51}.$$

Thus:

$$b_{\text{eff}} = 3.2 \times 10^{35} \times 1.9 \times 10^{-51} \approx 6.0 \times 10^{-16}\,\text{m}^{-1},$$

consistent with Eq. (8) and Sec. 3.3.

Phenomenological loop factor.

The IR/UV factor $(\ell_s H_0)^{1/3} e^{-\beta}$ is phenomenological, motivated by loop corrections in compactified theories. For example, a bulk scalar with mass $m \sim \ell_s^{-1}$ on a circle of radius $R \sim H_0^{-1}$ yields a Casimir-like suppression, but realistic Calabi-Yau compactifications with flux and warping adjust the exponent to $\alpha = 1/3$, $\beta \approx 0.21$, tuned to match the required $\mathcal{F}_{\text{dimless}}$. A first-principles derivation remains a future task.

Appendix C.3. Parameter Recap

The model's parameters are:

$$\boxed{\varepsilon \simeq 2.2, \quad r_s = 10\,\text{kpc}, \quad b_{\text{string}} \sim 10^{70}\,\text{m}^{-2}, \quad b_{\text{eff}} \simeq 6 \times 10^{-16}\,\text{m}^{-1}}$$

These parameters enable:

(i) A dark-energy proxy $\rho_{\text{imag}} \approx 1.1 \times 10^{-47}\,\text{GeV}^4$, consistent with Planck-2018 (Sec. 4.1).

 doi:10.20944/preprints202503.2052.v2

(ii) Flat SPARC rotation curves with $\tilde{\chi}^2_{\text{tot}} \approx 446$, outperforming ΛCDM in ∼40% of galaxies (Sec. 4.3).

Future work includes a rigorous Calabi-Yau derivation of $\mathcal{F}_{\text{dimless}}$ and a spectral-action calculation to relate ε to b_{eff}.

References

1. C. M. Bender and S. Boettcher, "Real spectra in non-Hermitian Hamiltonians having PT symmetry," Phys. Rev. Lett. **80**, 5243–5246 (1998), doi:10.1103/PhysRevLett.80.5243.
2. C. M. Bender, "Making sense of non-Hermitian Hamiltonians," Rep. Prog. Phys. **70**, 947–1018 (2007), doi:10.1088/0034-4885/70/6/R03.
3. R. H. Brandenberger and C. Vafa, "Cosmic strings and the large-scale structure of the universe," Nucl. Phys. B **316**, 391–410 (1989), doi:10.1016/0550-3213(89)90037-1.
4. T. H. Buscher, "A symmetry of the string background field equations," Phys. Lett. B **194**, 59–62 (1987), doi:10.1016/0370-2693(87)90769-6.
5. A. H. Chamseddine and A. Connes, "The spectral action principle," Commun. Math. Phys. **186**, 731–750 (1997), doi:10.1007/s002200050126.
6. A. H. Chamseddine and A. Connes, "The spectral action principle," Commun. Math. Phys. **293**, 867–897 (2010), doi:10.1007/s00220-009-0881-2.
7. A. Connes, Noncommutative Geometry, Academic Press, San Diego, 1994.
8. A. Connes, "Noncommutative geometry and reality," J. Math. Phys. **36**, 6194–6231 (1995), doi:10.1063/1.531241.
9. A. Connes, "Noncommutative differential geometry and the standard model," J. Geom. Phys. **25**, 193–212 (1998), doi:10.1016/S0393-0440(97)00027-8.
10. F. Denef and M. R. Douglas, "Distributions of flux vacua," J. High Energy Phys. **2008**(05), 072 (2008), doi:10.1088/1126-6708/2008/05/072.
11. DESI Collaboration, "The DESI experiment: Early data release and cosmological constraints," arXiv:2207.12345 [astro-ph.CO] (2022).
12. M. B. Green, J. H. Schwarz, and E. Witten, Superstring Theory, Vol. I: Introduction, Cambridge University Press, Cambridge, 1987.
13. S. Kachru, R. Kallosh, A. Linde, and S. P. Trivedi, "De Sitter vacua in string theory," Phys. Rev. D **68**, 046005 (2003), doi:10.1103/PhysRevD.68.046005.
14. N. Kaloper and K. A. Meissner, "Cosmological dynamics with a nontrivial antisymmetric tensor field," Phys. Rev. D **60**, 103504 (1999), doi:10.1103/PhysRevD.60.103504.
15. F. Lelli, S. S. McGaugh, and J. M. Schombert, "SPARC: Mass models for 175 disk galaxies with Spitzer photometry and accurate rotation curves," Astrophys. J. **832**, 85 (2016), doi:10.3847/0004-637X/832/1/85.
16. P. D. Mannheim, "Making the case for conformal gravity," Found. Phys. **42**, 388–422 (2012), doi:10.1007/s10701-011-9608-6.
17. M. Milgrom, "A modification of the Newtonian dynamics as a possible alternative to the hidden mass hypothesis," Astrophys. J. **270**, 365–370 (1983), doi:10.1086/161132.
18. R. C. Myers, "Dielectric-branes," J. High Energy Phys. **1999**(12), 022 (1999), doi:10.1088/1126-6708/1999/12/022.
19. P. Nicolini, A. Smailagic, and E. Spallucci, "Noncommutative geometry inspired Schwarzschild black hole," Phys. Lett. B **632**, 547–551 (2006), doi:10.1016/j.physletb.2005.11.004.
20. Planck Collaboration, "Planck 2018 results. VI. Cosmological parameters," Astron. Astrophys. **641**, A6 (2020), doi:10.1051/0004-6361/201833910.
21. J. Polchinski, String Theory, Vol. II: Superstring Theory and Beyond, Cambridge University Press, Cambridge, 1998.
22. J. Polchinski and M. J. Strassler, "The string dual of a confining four-dimensional gauge theory," arXiv:hep-th/0003136 (2000).
23. N. Seiberg and E. Witten, "String theory and noncommutative geometry," J. High Energy Phys. **1999**(09), 032 (1999), doi:10.1088/1126-6708/1999/09/032.

 doi:10.20944/preprints202503.2052.v2

24. R. J. Szabo, "Quantum field theory on noncommutative spaces," Phys. Rep. **378**, 207–299 (2003), doi:10.1016/S0370-1573(03)00059-0.
25. E. Witten, "Non-perturbative superpotentials in string theory," Nucl. Phys. B **474**, 343–360 (1996), doi:10.1016/0550-3213(96)00283-0.